International Journal of Technology

http://ijtech.eng.ui.ac.id

Research Article

Biofuel Production from Waste Cooking Oil over Copper-Metal-Organic Framework/ Potassium Oxide Catalyst for Alternative Bioenergy

Tri Widjaja[1*], Ali Altway[1], Shofia Khoirunnisa[1], Dinda Amelia Nurhanifa[1], Mahfud Mahfud[1], Hendro Juwono[2], Joni Prasetyo[3], Deliana Dahnum[3], Aisyah Alifatul Zahidah Rohmah[4]**

[1]Chemical Engineering Department, Sepuluh Nopember Institute of Technology, Sukolilo, Surabaya 60111, Indonesia

[2]Chemistry Department, Sepuluh Nopember Institute of Technology, Sukolilo, Surabaya 60111, Indonesia

[3]Research Center for Molecular Chemistry, National Research and Innovation Agency (BRIN), Tangerang Selatan 15314, Indonesia

[4]Chemical Engineering Department, East Java Veterans National Development University, Gunung Anyar, Surabaya 60294, Indonesia

[*]Corresponding author: tri.widjaja@its.ac.id; Tel.: +6282132279449

[**]Corresponding author: deli001@brin.go.id; Tel.: +6281586840420

Abstract: This study investigated the synthesis and application of Cu-MOF/K_2O catalysts for pyrolytic catalytic cracking (PCC) of waste cooking oil (WCO) to produce biofuels. Cu-MOF/K_2O catalysts were synthesized via a facile temperature method by incorporating copper as the metal center and 2-methylimidazole as the organic ligand with varying K_2O concentrations (3, 5, and 10 wt%), followed by thermal treatment at 500 ºC. WCO was reacted under atmospheric pressure with N_2 gas at various temperatures to produce an oil-liquid product (OLP). Characterization by FT-IR and XRD confirmed the decomposition of Cu-MOF into CuO and Cu_2O, while XRF revealed the increase in K_2O concentration in Cu-MOF/K_2O as a result of varying the base. SEM imaging demonstrated a uniform particle size distribution in Cu-MOF/K_2O, while the BET surface area analysis indicated a reduction in the surface area due to K_2O incorporation. The NH_3 and CO_2-TPD confirmed the coexistence of several types of acidic and basic sites in the catalyst. GC-MS analysis of OLP revealed a significant enhancement in hydrocarbon content following PCC, with Cu-MOF/10-K_2O achieving a maximum hydrocarbon yield exceeding >99.9% at 400 °C, containing 53% biogasoline, 29% biokerosene, and 18% green diesel, indicating high selectivity toward transportation-range fuels. This study highlights the potential of a cost-effective catalyst, Cu-MOF/K_2O, in advancing sustainable biofuel production, thereby reducing reliance on fossil fuels and promoting environmental sustainability.

Keywords: Biofuel; Cu-MOF/K_2O; Deoxygenation; Pyrolytic catalysis cracking; Waste cooking oil

1. Introduction

Since the Industrial Revolution, global energy consumption has predominantly relied on fossil fuels, significantly contributing to environmental degradation and climate change. In recent years, the volatility of crude oil prices peaked at $130 per barrel in 2022 and in 2023-2025 around $70-$85 per barrel in 2023–2025, which is lower than that in 2022 (French, 2024; Associates, 2020). Geopolitical factors continued to trigger short-term price fluctuations. These reasons have underscored the urgent need for alternative energy solutions. Global primary energy consumption increased by approximately 630 EJ in 2024. This growth of around 2.2% reflects an increased contribution from renewable energy sources (97 EJ) and natural gas (149

https://doi.org/10.14716/ijtech.v17i2.8009
Received August 2025; Revised December 2025; Accepted January 2026

EJ). Renewable energy is anticipated to play a pivotal role, with global demand expected to be double by 2040 (Garside, 2019). Conflicts such as the Russia–Ukraine war, escalating tensions in the Middle East, and disruptions along key maritime routes have repeatedly triggered energy price volatility and oil and gas supply chain uncertainty. These geopolitical risks have amplified market instability, reinforcing the urgency to diversify energy sources. The transition from fossil fuels to sustainable energy sources is crucial, and biofuels derived from biological materials, such as triglycerides or carboxylic acids, are a viable renewable energy alternative.

Waste cooking oil (WCO) is a particularly noteworthy biofuel feedstock because of its potential for producing liquid fuels and high-value chemicals. The global annual WCO generation is estimated at 220 million tons (Cárdenas et al., 2021; Long et al., 2020). Indonesia, one of the largest palm oil producers globally, contributes approximately 45.5 million tons, or 59% of the global palm oil demand (Dewi and Agarta, 2023). As of December 31, 2023, Indonesia's annual palm oil consumption for food purposes reached 10.3 million liters, correlating with significant WCO generation (Ulfa, 2022). The abundance of WCO in Indonesia is primarily attributed to its large population and culinary traditions, where fried foods are a staple. High-quality WCO is generally obtained from upscale restaurants, while street vendors are the primary source of low-quality WCO. Using WCO as a feedstock provides significant environmental advantages, including reducing waste management challenges and minimizing environmental pollution.

Biofuels can be produced through various routes, including transesterification, esterification, and cracking processes. Among these methods, pyrolytic catalytic cracking (PCC) has become a promising approach for converting WCO into biofuels. PCC integrates thermal pyrolysis with catalytic upgrading to efficiently convert triglycerides and free fatty acids into fuel-range hydrocarbons under mild conditions at atmospheric pressure, without the need for purging gas as required in hydrocracking or hydrotreating (Baharudin et al., 2020). Nevertheless, the conversion of WCO presents challenges due to its high oxygen content and the presence of contaminants. During PCC, long-chain molecules are broken down into smaller hydrocarbons through molecular bond cleavage and free radical propagation, resulting in the formation of more stable products. The efficiency of this process can be significantly enhanced by using an appropriate catalyst, which promotes targeted reactions and improves biofuel yield (Laksmono et al., 2013). Typically, PCC is conducted at elevated temperatures in the range of 400°C–600°C, which are favorable for effective cracking reactions. According to previous studies, the optimal temperature for producing green biofuels with higher yields is 525°C using CaO-MgO catalysts, while another study identified 475°C as the optimal temperature when using ZrO_2 catalysts (Chueaphetr et al., 2023; Wakoc et al., 2018). Further research demonstrated that the highest yield was achieved at 400°C using activated carbon as the catalyst (Banchapattanasakda et al., 2023). Although acidic catalysts, such as HZSM-5 and MCM-41, have traditionally been used as catalysts, they are prone to coke formation and catalyst deactivation. Accordingly, the synthesis of catalysts exhibiting reduced acidity and improved basicity could be considered.

The use of precious metals, such as Pd, Pt, and Ru, in support materials has been reported to be effective in converting fatty acid-based vegetable oil (Mohammed et al., 2022; Edeh et al., 2021; Snare et al., 2006). In addition, transition metal oxides (including Ni, Co, Mo, W, and Zn) have been extensively investigated in the deoxygenation of fatty acids (Prasetyo et al., 2026). These metal oxides have exhibited a significant capability to facilitate oxygen removal and carbon chain cleavage with excellent selectivity to produce hydrocarbon products (Jeon et al., 2020; Yıldız et al., 2020; Srifa et al., 2015). Additionally, owing to their high surface area and abundance of active sites, metal-organic frameworks (MOFs), a class of porous crystalline materials comprising metal ions and organic ligands, have gained attention for catalytic applications. MOFs demonstrate potential as self-sacrificial templates and precursors for synthesizing diverse carbon-based materials, which is attributed to their exceptionally high surface area, substantial pore volume, and remarkable structural and compositional tunability (Shen et al., 2016). The sacrificial template generated from the thermal decomposition of MOF has been reported to produce various carbon-based nanomaterials, including metal/metal oxide decorated porous

carbons (Sun and Xu, 2014). The flexibility in selecting metal ions and organic ligands enables the design of MOF-based sacrificial templates with structures and properties tailored to meet the needs of specific applications, especially to prevent the aggregation of metal nanoparticles or metal oxides in the thermal process (Shen et al., 2016).

This study aimed to synthesize a cost-effective MOF-derived copper oxide catalyst and evaluate its catalytic performance for the conversion of WCO into hydrocarbon biofuels. To the best of our knowledge, this is the first report on the application of MOF-derived copper oxide as a catalyst for the deoxygenation of waste feedstocks. In this study, a novel strategy for MOF synthesis was employed using 2-methylimidazole as the organic linker, in contrast to the more commonly adopted benzene-1,4-dicarboxylic acid (BDC) ligand and DMF solvent system typically used in solvothermal approaches (Jamil et al., 2020). In addition, the basicity of the catalyst was tuned by K_2O incorporation to form Cu-MOF/K_2O, aiming to enhance the deoxygenation efficiency and hydrocarbon selectivity. Remarkably, our findings show that the use of a single metal oxide, Cu-MOF/K_2O, enables the conversion of WCO to biofuel with notable yield and selectivity, without the need for an external hydrogen input. These findings underscore the potential for improving energy efficiency, reducing operational costs, and enhancing safety, particularly in large-scale applications.

2. Materials and Methods

2.1 Materials

The materials used to produce Cu-MOF, such as copper (II) sulfate anhydrous ($CuSO_4.5H_2O$), methanol (MeOH) (Sigma, 99%), 2-methylimidazole (Sigma, 99%), potassium acetate (CH_3COOK) (Sigma, 99%), and deionized (DI) water, were used without further purification. The raw material, WCO, was collected from street vendors in Surabaya, Indonesia, to ensure that it was a representative feedstock for biofuel production.

2.2 Catalyst synthesis and characterization

Cu-MOF/K_2O was prepared according to a previously reported method with some modifications (Putri et al., 2025; Baharudin et al., 2020). Cu-MOF was synthesized at room temperature (27 °C) using a metal-to-organic molar ratio of 1:2, with $CuSO_4.5H_2O$ as the metal precursor and 2-methylimidazole as the organic linker. In the separate beakers, $CuSO_4.5H_2O$ was dissolved in distilled water, while 2-methylimidazole was dissolved in methanol. The two solutions were then mixed and stirred overnight at 300 rpm under ambient temperature, resulting in the formation of a precipitate. Subsequently, this precipitate was collected via centrifugation at 5000 rpm for 5 min and dried at 100 °C overnight to produce Cu-MOF. Potassium loading on the Cu-MOF catalyst was performed using the wet impregnation technique, with concentrations of 3%, 5%, and 10% by weight. A potassium solution prepared by dissolving CH_3COOK in distilled water at an incipient wetness volume of 5 mL/g of Cu-MOF. The solution was added slowly to the catalyst under continuous stirring, followed by drying at 80°C overnight and calcination at 500°C for 5 h, yielding Cu-MOF/3-K_2O, Cu-MOF/5-K_2O, and Cu-MOF/10-K_2O potassium concentrations of 3%, 5%, and 10%, respectively.

The characterization of the synthesized catalysts involved several analytical techniques. X-ray Diffraction (XRD) was employed to investigate the crystallographic structure using a D8 Advance instrument (Bruker, Germany), scanning across a 2θ range from 5° to 70° at a speed of 0.05° per minute with CuKa-filtered radiation. The resulting XRD patterns and peaks were compared to JCPDS (Joint Committee on Powder Diffraction Standards) references for identification. Fourier Transform Infrared (FTIR) spectroscopy, performed with a Nicolet iS5 spectrometer (Thermo Scientific, USA), was used to identify functional groups in the Cu-MOF/K_2O samples, with a scanning range of 650 cm^{-1} to 4000 cm^{-1} and a resolution of 4 cm^{-1}. The morphological and elemental composition of the catalysts was examined via Scanning Electron Microscopy (SEM) combined with Energy Dispersive Spectroscopy (SEM-EDS, JEOL-2100F

SEM), where the samples were placed on a carbon-coated copper grid.

Thermogravimetric Analysis (TGA) was conducted using a TGA 5500 instrument (TA Instruments, USA) to determine the thermal stability of the synthesized materials. The analysis involved heating the samples from 20°C to 800°C at 5°C per minute to monitor the weight loss percentage. Brunauer, Emmett, and Teller's (BET) analysis assessed the materials" specific surface area, pore volume, and size. The acidity of the catalysts was evaluated using Ammonia-Temperature Programed Desorption (NH_3-TPD) via the Chemisorb 2750 system (Micromeritics), while the basicity of the catalysts was measured using Carbon dioxide-Temperature Programed Desorption (CO_2-TPD) by the Autochem system.

2.3 Biofuel Production and Product Analysis

The biofuel production process was performed using the PCC method in a fixed-bed reactor made of stainless steel with a capacity of 600 mL, integrated with a condenser to condense the product (Figure 1).

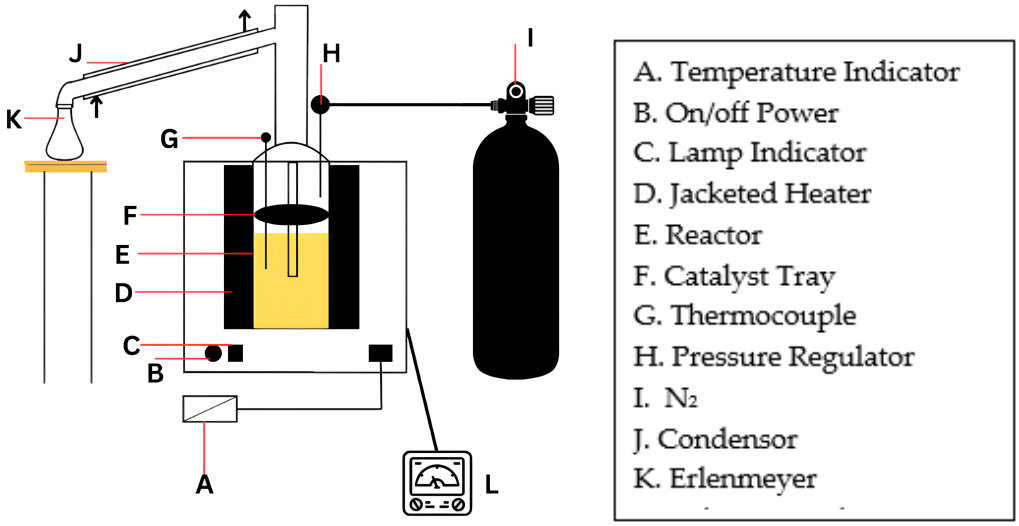

Figure 1 Schematic of Pyrolytic Catalysis Cracking (PCC) equipment

Prior to the PCC process, WCO was pretreated using commercial bleaching earth to remove impurities. The oil was heated to boiling temperature, and then 100 g of bleaching earth was added per 2 L of oil. After thorough mixing, the mixture was cooled to room temperature and filtered to obtain treated WCO. This treated oil was then transferred into the reactor, followed by the addition of 5 wt% of catalyst, which was placed in the catalyst tray. The reactor was heated to the desired temperature under atmospheric pressure with a continuous nitrogen gas flow maintained at 2 bar. The treated WCO was converted into a vapor phase by passing through the pyrolytic zone. The pyrolysis vapor was condensed into the liquid phase, resulting condensate of oil-liquid product (OLP). The OLP was filtered using filter paper to separate impurities from oil and a separatory funnel to remove water, and then analyzed using Gas Chromatography-Mass Spectrometry (GC-MS), Agilent 19091S-433 with a DB-5MS capillary column (Agilent 7890A) with an HP-5 capillary column (30 m × 0.25 mm × 0.25 μm). The yield of OLP, the distribution of each product in OLP, and biofuel product selectivity (biogasoline, biokerosene, and green diesel) were calculated according to a previous report without overlapping the chain size range using the following equations (Scaldaferri and Pasa, 2019) :

$$\text{Yield of OLP } (\%) = \left(\frac{\text{Mass of OLP collected}}{\text{Mass of feed}}\right) \times 100\% \quad (1)$$

$$\text{Distribution of each product in OLP } (\%) = \left(\frac{\text{Area each product in OLP}}{\text{Total area of OLP}}\right) \times 100\% \quad (2)$$

$$\text{Biogasoline selectivity } (\%) = \left(\frac{\text{Total area of C5}-\text{C11 in OLP}}{\text{Total area of hydrocarbon in OLP}}\right) \times 100\% \quad (3)$$

$$\text{Biokerosene selectivity } (\%) = \left(\frac{\text{Total area of C12}-\text{C16 in OLP}}{\text{Total area of hydrocarbon in OLP}}\right) \times 100\% \quad (4)$$

$$\text{Green diesel selectivity } (\%) = \left(\frac{\text{Total area of C17}-\text{C20 in OLP}}{\text{Total area of hydrocarbon in OLP}}\right) \times 100\% \quad (5)$$

3. Results and Discussion

3.1 Characterization of the synthesized catalyst

Fourier Transform Infrared (FT-IR) spectroscopy was used to confirm the functional groups that existed in the synthesized material. The FT-IR results for the synthesized Cu-MOF and Cu-MOF/K_2O, including 2-methylimidazole as reference, are presented in Figure 2 (a). As shown in the FTIR spectra, Cu-MOF exhibits a sharp peak that mainly corresponds to 2-methylimidazole. The peak observed in the range of 2700-3200 cm^{-1} in Cu-MOF was associated with the aromatic and aliphatic C-H asymmetric stretching vibrations of imidazole. The band at 1572 cm^{-1} corresponds to the C=N stretch mode. The peaks in the range of 1400 – 1300 cm^{-1} attributed to the entire ring stretching, while the band at 1152 cm^{-1} could be assigned to C-N bending vibration (Zhang et al., 2018). Based on the spectra, we suggest that 2-methylimidazole was retained in Cu-MOF. However, after impregnation with K_2O, a significant change was observed in the FT-IR results of the Cu-MOF/10-K_2O catalyst. Additionally, the sharp peaks at 1104 cm-1, assigned to out-of-plane bending of the imidazole ring were remained only (Binaeian et al., 2019). The incorporation of K_2O induces significant structural changes, leading to the decomposition of the Cu-MOF framework.

The structural characteristics of the synthesized materials investigated by X-ray Diffraction (XRD) analysis. Figure 2 (b) presents the XRD pattern of Cu-MOF, showing diffraction peaks at 35.62° and 36.55°, which correspond to CuO (002) and Cu_2O (111), respectively (Yang et al., 2016) y (Battauz et al., 2025;Veisi et al., 2021; Murthy et al., 2021)). Several unidentified peaks in Cu-MOF are likely attributed to the incomplete decomposition of Cu-MOF into CuO or Cu_2O, which is attributed to the stretching vibrations characteristic of 2-methylimidazole observed by FT-IR analysis. Interestingly, the addition of a potassium compound or K_2O in Cu-MOF appears to facilitate the formation of Cu-metal oxide phases. As shown in the XRD pattern of MOF/3-K_2O, the distinct peaks at 35.67°, 38.87°, and 61.5° correspond to CuO (002), (111), (-113), while the additional peaks at 36.6° and 42.5° confirmed the presence of Cu_2O (111) and (200). Both CuO and Cu_2O were similarly observed in Cu-MOF/5-K_2O. Moreover, a high concentration of K_2O promote the transformation of CuO to Cu_2O, as shown in the Cu-MOF/10-K_2O diffraction pattern. Based on the XRD data, we concluded that the Cu-MOF transformed into CuO and Cu_2O after being calcined at 500 °C. The increased potassium concentration promoted the crystal structure change from CuO to Cu_2O, as shown in Cu-MOF/5-K_2O and Cu-MOF/10-K_2O. The K_2O peak could not be observed in the XRD analysis, possibly due to the low potassium concentration added to the Cu-MOF. However, the X-Ray Fluorescence (XRF) analysis confirmed the presence of potassium or K_2O on the surface of the impregnated Cu-MOF. As shown in Table 1, increasing the potassium content during the impregnation process resulted in a corresponding increase in the K_2O concentration of the synthesized catalysts.

To investigate the effect of K_2O impregnation on the specific surface area, pore volume, and pore diameter of the synthesized Cu-MOF catalyst, Brunauer–Emmett–Teller (BET) analysis was conducted. Table 2 presents the physical properties of Cu-MOF and Cu-MOF/K_2O obtained through N_2 physisorption analysis. Cu-MOF exhibits a surface area of 435 m^2g^{-1}, which decreases to 405 m^2g^{-1}, 428 m^2g^{-1}, and 397 m^2g^{-1} for the MOF/3-K_2O, MOF/5-K_2O, and MOF/10-K_2O catalysts, respectively. The decrease in surface area is likely due to the blocking

of small pores by potassium oxide particles during the impregnation process (Jawad et al., 2020). However, this reduction in the specific surface area does not follow a linear relationship with the pore volume and diameter. In the case of Cu-MOF/10-K_2O, the pore volume from 0.409 cm^3g^{-1} to 0.374 cm^3g^{-1}, while the pore diameter increased from 3.763 to 3.772 nm. This can be attributed to the opening of new pores due to the impregnation and calcination processes; however, these newly formed pores are simultaneously closed by potassium oxide in the Cu-MOF/10-K_2O catalyst. Consequently, the pore volume does not increase in tandem with the pore diameter (Rodiansono et al., 2007). This phenomenon is also observed in Cu-MOF/10-K_2O, where the pore volume decreases but the pore diameter increases compared to Cu-MOF. The experimental results indicate that the use of imidazole as an organic solvent in Cu-MOF synthesis yields a specific surface area of 435 m^2g^{-1}, significantly higher than that of previous studies on Cu-MOF synthesis that used benzene-1,4-dicarboxylic acid (BDC) as linkers, which resulted in a surface area of 118 m^2g^{-1} (Jamil et al., 2020).

Table 1 Elemental analysis of the synthesized catalyst using XRF

Oxide form	Synthesized catalyst			
	Cu-MOF	Cu-MOF/3-K_2O	Cu-MOF/5-K_2O	Cu-MOF/10-K_2O
CuO	99.87%	98.53%	97.81%	92.66%
K_2O	0.13%	1.47%	2.19%	7.34%

Table 2 Textural properties of the synthesized Cu-MOF and Cu-MOF/K_2O through the BET analysis

Catalyst	Specific surface area (SA_{BET}) (m^2g^{-1})	Pore volume (V_{pore}) (cm^3g^{-1})	Pore diameter (D_{pore}) (nm)
Cu-MOF	435	0.409	3.763
Cu-MOF/3-K_2O	405	0.409	4.041
Cu-MOF/5-K_2O	428	0.401	3.750
Cu-MOF/10-K_2O	397	0.374	3.772

To examine the morphology of the synthesized Cu-MOF and Cu-MOF/K_2O catalysts, Scanning Electron Microscopy (SEM) analysis was conducted. As shown in Figures 3(a) and (b), the morphology of the Cu-MOF before impregnation shows oval or granular particles. The particle size distribution is nonuniform, with some particles appearing more significant and compact, indicating partial aggregation. However, the Cu-MOF particles are well-defined. In contrast, Figures 3(c) and (d) show a rougher surface with more aggregated particles. The SEM analysis confirms that the impregnation of K_2O leads to increased aggregation and rougher surface morphology in Cu-MOF/10-K_2O, resulting in changes in the texture and particle size distribution that might enhance the catalytic properties. This aligns with the observed polyhedral crystal structures in Co-MOF-74, where the excellent catalytic performance was confirmed by the aggregated morphology (Jiang et al., 2016).

The thermal behavior of the synthesized catalyst was evaluated through Thermogravimetric Analysis (TGA) under a nitrogen atmosphere within the temperature range of 50-800 °C. For Cu-MOF/5-K_2O, significant mass losses were observed in two distinct peaks, as shown in Figure S1. The first peak occurred between 50 °C and -400 °C and showed a weight reduction of approximately 6.88 wt%, corresponding to water removal, removal of impurities, or unreacted 2-methylimidazole. The second peak, observed between 650 °C and -750 °C, shows a mass loss of 6.75 wt%, which is associated with the decomposition of potassium moieties, leading to the release of gases such as H_2 and O_2 (Chueaphetr et al., 2023). Higher K_2O impregnation levels increased the residual mass at the end of the TGA process, reflecting enhanced thermal stability. The calcination procedure at 500 °C for 5 h, which promotes the complete breakdown of KOH and the formation of K_2O, is responsible for this enhanced stability (Hoque et al., 2022).

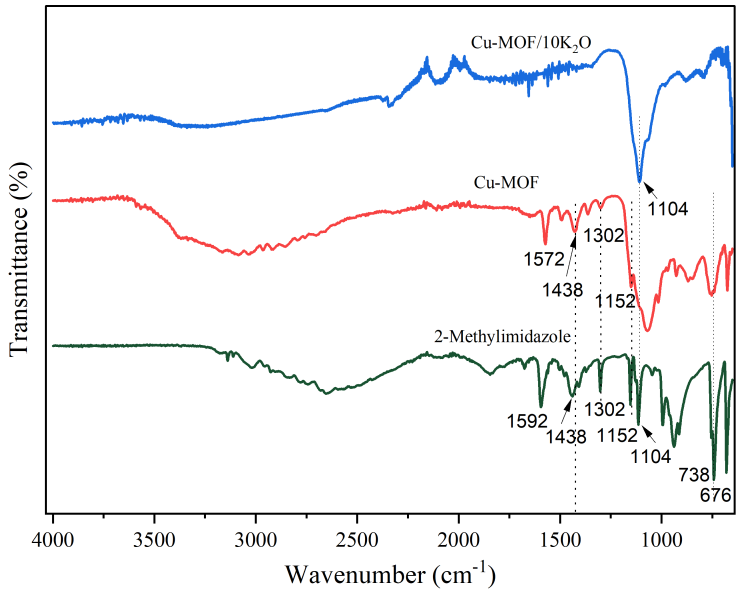

(a)

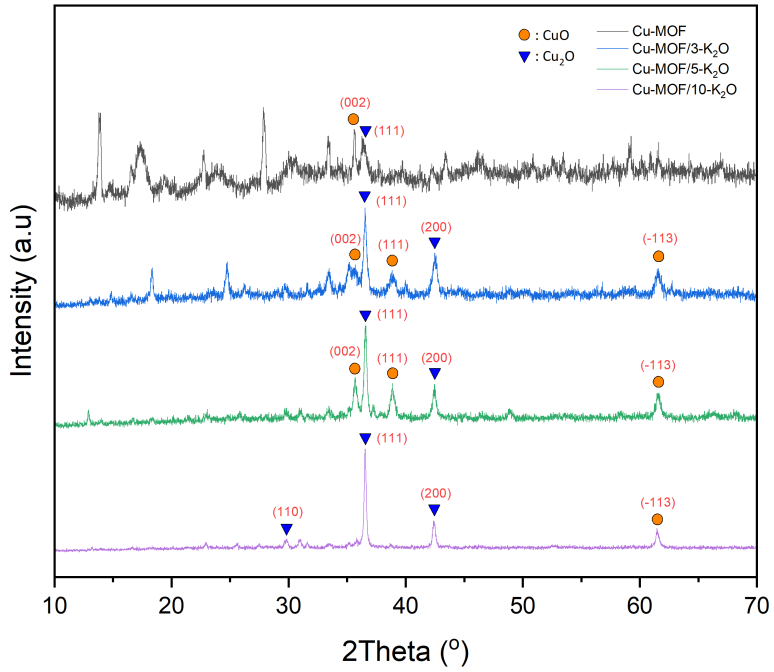

(b)

Figure 2 (a) Infrared spectra of Cu-MOF and Cu-MOF/10-K_2O compared with 2-Methylimidazole and (b) X-ray diffraction pattern of the Cu-MOF/K_2O series.7Cu-7Zn-3.5Ag, and (d) Sn-0.7Cu-7Zn-4Ag

The endothermic process further enhances the thermal resilience of the material, which requires heat to convert potassium into its oxide form (K_2O) (Chueaphetr et al., 2023). The structural stability in the SEM examination in Figure 3, where K_2O impregnation results in more aggregated and rougher surface morphologies, correlates with the residual mass at higher temperatures. These structural changes preserve the material's structural integrity and func-

tionality under operating conditions by strengthening the material's resistance to thermal deterioration. The substantial weight loss at 650 °C shows good thermal stability, making it suitable for high-temperature applications such as biofuel generation. Increased thermal stability ensures constant performance and selectivity over extended use by implying more prolonged catalyst activity, better durability, and lower regeneration frequency. These findings emphasize the role of K_2O impregnation in optimizing the thermal and catalytic properties of Cu-MOF catalysts for sustainable energy applications.

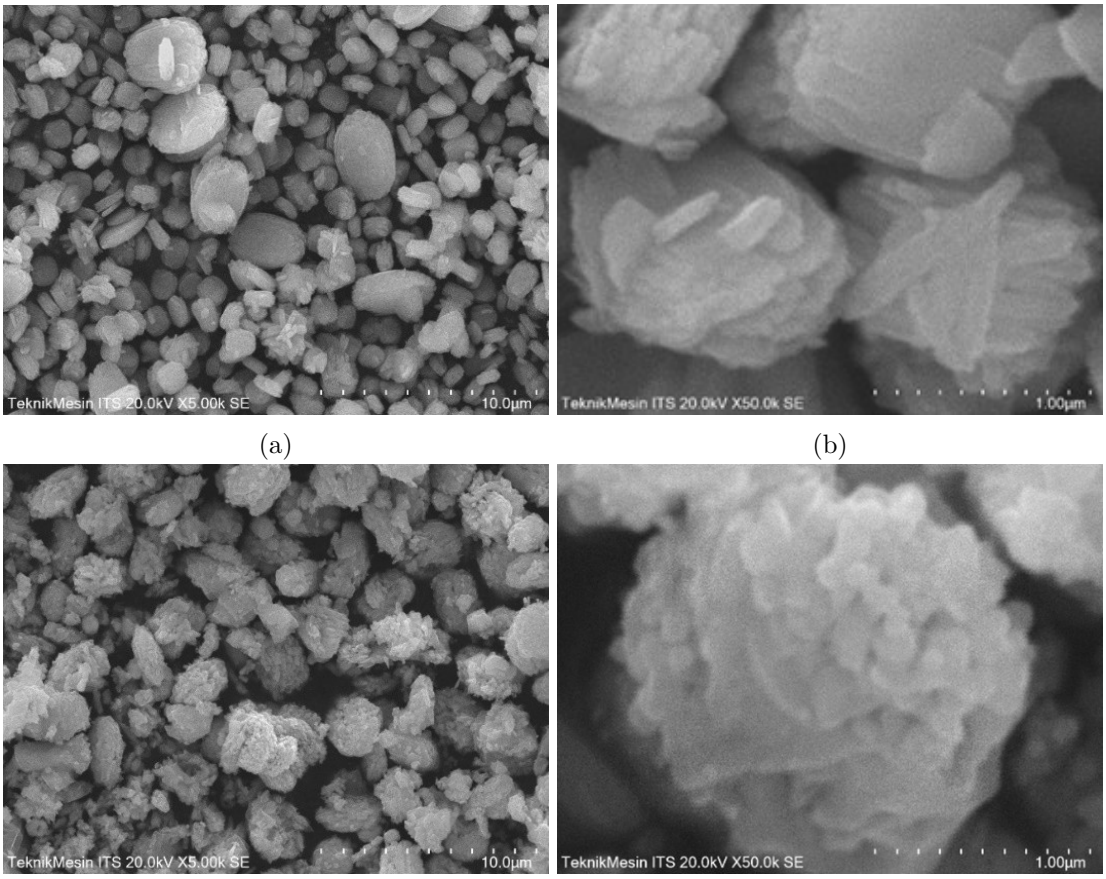

Figure 3 (SEM images at different magnifications of (a) Cu-MOF 10 μm, (b) Cu-MOF 1 μm, (c) Cu-MOF/K_2O 10 μm, and (d) Cu-MOF/10-K_2O 1 μm

3.2 Production of biofuel with PCC of WCO

According to GC-MS composition analysis, WCO contains high levels of fatty acids, primarily oleic acid (C18:1) and linoleic acid (C18:2) (Table 3, Figure S2a). Fatty acids are incorporated within the triglyceride structure, which serves as the primary hydrocarbon in WCO.

Table 3 Distribution of fatty acid chains in the Waste Cooking Oil (WCO)

Component	(%)
Myristic acid (14:0)	0.24
Palmitic acid (16:0)	9.84
Stearic acid (18:0)	4.44
Oleic acid (18:1)	33.83
Linoleic acid (18:2)	32.64
Others	19.01

The reaction was performed continuously in a fixed-bed reactor with Cu-MOF, Cu-MOF/3-K_2O, Cu-MOF/5-K_2O, and Cu-MOF/10-K_2O catalysts placed in the pyrolytic zone using an 80-mesh sieve. WCO is vaporized during the PCC process as it passes through the pyrolytic zone. This constant increase in the volume of both reactants and products within the fixed-bed reactor is observed throughout the process. The influences of reaction time, reactor heating rate, and temperature on OLP products were systematically evaluated to optimize the performance of the catalytic system reaction.

3.2.1 Optimization of the Reaction Time of a Fixed-Bed Reactor

Figure 4(a) shows the distribution of OLP components obtained using Cu-MOF/10-K_2O catalyst at varying reaction times. GC-MS analysis revealed that the OLP predominantly contains saturated alkanes, certain unsaturated alkenes, cyclic hydrocarbons, and trace levels of glycerol derivatives (Figure S2b). Interestingly, the control experiment conducted without the addition of a catalyst confirmed the significant presence of unconverted fatty acids in OLP, clearly demonstrating the role of the catalyst in achieving efficient deoxygenation (Table S1). A WCO, shown in Figure 4(a) as 0 min reactions, contains a high fatty acid concentration with less saturated and unsaturated hydrocarbon traces. At a reaction time of 30 min, WCO conversion was incomplete, leaving a considerable amount of fatty acid in the product. As the reaction time increased, the amounts of fatty acids gradually decreased and converted into saturated hydrocarbons at higher concentrations, with a decrease in unsaturated hydrocarbons. Saturated hydrocarbons, primarily long-chain alkanes, dominated the hydrocarbon components formed at a reaction time of 60 min. However, after 60 minutes, the fraction of saturated hydrocarbons began to decline after 60 min,, and additional compounds appeared at 90 min due to side reactions such as thermal pyrolysis and decomposition of organic compounds into gaseous products. At 120 minutes, the concentration of unsaturated hydrocarbons increased significantly at 120 min, that other products react to form alkenes with prolonged reaction time. In addition, the yield of OLP increased gradually with reaction time, from 10% to 30% for reaction times of 30 and 120 min, respectively. Nevertheless, according to the results, a reaction time of approximately 60 min was considered the best condition.

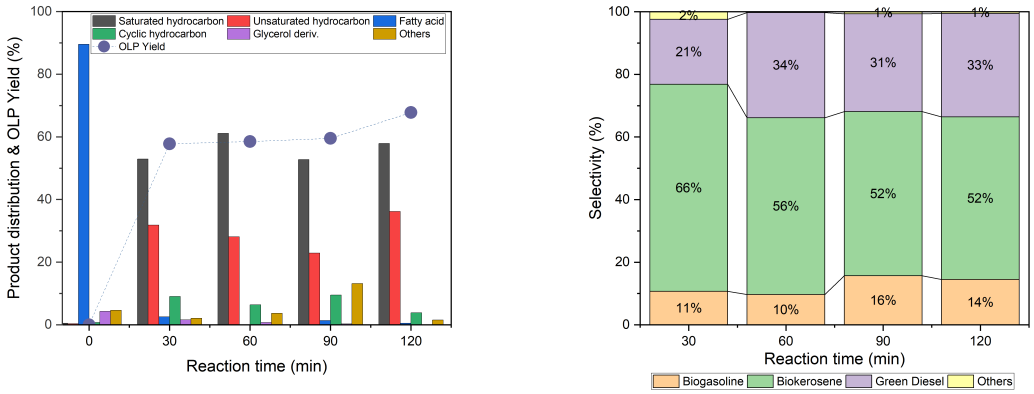

(a) (b)

Figure 4 (a) Product distribution and (b) biofuel selectivity of OLP on time reaction. Reaction Cond.: 272 g WCO, 15 g Cu-MOF/10-K_2O, 370 °C

The biofuel selectivity in the OLP was categorized into three hydrocarbon fractions based on carbon number ranges: biogasoline (C5-C11), biokerosene (C12-C16), and green diesel (C17-C20) (Figure 4(b)). The other component was observed for hydrocarbons with a long carbon chain >C20. Accordingly, at a reaction time of 30 min, kerosene dominated the obtained product. However, the amount of fatty acid still existed in the OLP, rendering the fatty acid conversion incomplete in the 30-min reaction. When the PCC reaction proceeded for 60 min, biogasoline,

biokerosene, and green diesel yielded 10%, 56%, and 34%, respectively. Biokerosene was found to be dominant in OLP products. Increasing the reaction time to 90- and 120-min results in a decrease in green diesel and bio-kerosene selectivity, whereas the biogasoline yield increases. This is possibly due to the cracking reaction that occurred during the prolonged reaction time. However, with the increase in reaction time, the selectivity of biofuel did not change significantly. Therefore, the reaction time for the PCC process was set at 60 min. For comparison, a previous study using a ZrO_2 catalyst reported optimal conditions at 475 °C with a reaction time of 120 min (Wakoc et al., 2018). In contrast, the synthesized catalyst in this study exhibited enhanced efficiency, achieving higher yields at lower reaction temperatures and shorter reaction times.

3.2.2 Optimization of the Heating Rate of a Fixed-Bed Reactor

The heating rate applied in a fixed-bed reactor might play an important role in the heating of WCO. Based on the results, OLP yields of 78.76% (4 °C/min) and 83.67% (8 °C/min) were achieved at a temperature of 400 °C with Cu-MOF/10-K_2O, indicating that a heating rate of 8 °C/min delivers the best performance. These findings align with previous cracking studies using heating rates of 10 °C/min and 20 °C/min, where no significant differences in yield were observed (Wakoc et al., 2018). Thus, a heating rate of 8°C/min, within the 10°C/min range, is optimal for the PCC process. Based on Figure 5, the product fraction shows that biokerosene has the most significant yield. At a heating rate of 4 °C/min, biogasoline, biokerosene, and green diesel had selectivities of 20%, 59%, and 20%, respectively. The other long-chain hydrocarbon products, around 1%, existed in the OLP product. The selectivity toward biokerosene and biogasoline increased to 23% and 61%, respectively, when the heating rate was increased to 8°C/min, accompanied by a reduction in green diesel selectivity. No other by-products were detected. This indicates that the heating rate could influence the composition of the OLP, as a higher rate of the cracking reactions produces shorter-chain hydrocarbons.

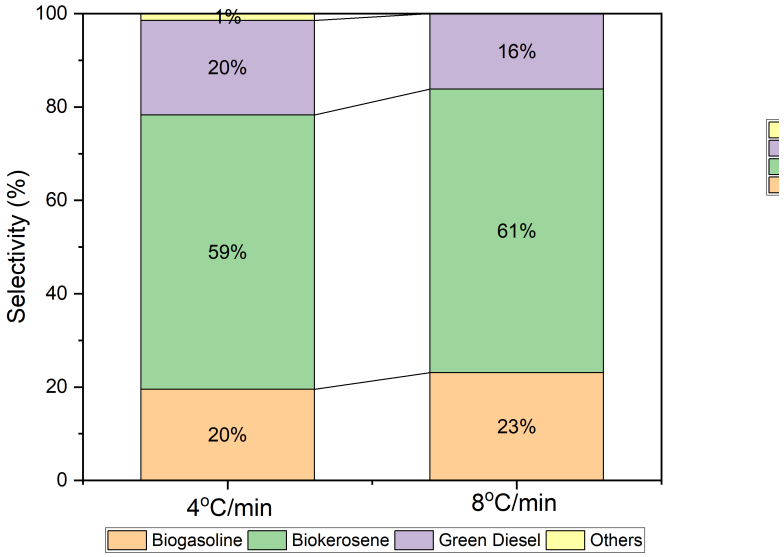

Figure 5 Effect of OLP biofuel selectivity on the heating rate of reactor performance optimization Reaction Cond.: 272 g WCO, 15 g Cu-MOF/10-K_2O, 400 °C

3.2.3 Effect of Reaction Temperature and K_2O on Biofuel Yield

According to the above discussion, the reaction was optimum for 1 h at a heating rate of 8 °C/min. In addition, the effect of temperature on the yield of OLP was examined at 370°C, 400 °C, and 430 °C. Figure 6(a) demonstrates that temperature plays a critical role in the OLP

yield. At 370°C, the yield reached 58.33% with the Cu-MOF/10-K_2O catalyst. Increasing the temperature to 400 °C resulted in a significant increase to 83.87%, while a further increase to 430 °C led to a decline in yield to 76.83%. This observed trend might be attributed to the optimization of conversion at 400 °C under equilibrium conditions, followed by a decrease in catalyst activity at higher temperatures. Therefore, 400 °C was identified as the optimal temperature for obtaining the maximum OLP. Figure 6(b)-(d) presents the OLP composition as influenced by the reaction temperature using the synthesized catalyst. The WCO initially exhibits a high content of oxygenated compounds, accounting for 98.47%, primarily fatty acids, contributing to its high acidity. Significant changes in the chemical composition of the OLP were observed after PCC.

As shown in Figure 6(b)-(d), the hydrocarbon content in OLP influenced by the reaction temperature. At 370 °C, the use of the synthesized catalysts led to the formation of smaller fatty acid compounds, indicating that long-chain fatty acids or triglycerides had been cracked. It resulted in higher oxygenated compounds in OLP, while the hydrocarbon was obtained at 10.38%, 13.64%, and 20.48% for Cu-MOF/3-K_2O, Cu-MOF/5-K_2O, and Cu-MOF/10-K_2O, respectively. An increase in the reaction temperature to 400 °C significantly enhanced the hydrocarbon production, yielding 95.90%, 96.05%, and >99.9% for the respective catalysts, respectively.. However, ketone compounds such as heptadecanone, pentadecanone, and tridecanone were detected in the OLP across all catalysts at 430 °C, that ketonization reactions likely occurred at this elevated temperature. Previous reports indicate that ketonization could proceed over metal-oxide catalysts containing acid-base properties under hydrogen-deficient conditions (Pikoli et al., 2025), considering that it might be present in the current catalytic system. Thus, 400 °C was determined to be the most favorable reaction temperature for optimal hydrocarbon production.

The PCC process occurs in two stages: WCO cracking by the thermal decomposition of triglycerides and fatty acid molecules yields an oxygenated product, followed by the reaction of the oxygenated product to form hydrocarbons (Chueaphetr et al., 2023). We predicted that the deoxygenation process that might occur was the decarbonylation and decarboxylation reaction. The decarbonylation reaction involves removing the carbonyl groups (C=O) from the oxygenated compound and releasing the carbon monoxide (CO). The decarboxylation reaction releases carbon dioxide (CO_2) by eliminating the carboxylate groups (COOH). Accordingly, XRD analysis reveals the presence of CuO and Cu_2O resulting from calcinated Cu-MOF in a synthesized catalyst that might contribute to the removal of oxygen in WCO (Ooi et al., 2019). Moreover, the acid sites, determined by the amount of NH_3 desorbed, reflect the strength and type of acid sites: desorption peaks in the 250°C–450°C range represent weak acid sites, 450°C–630°C correspond to medium acid sites, and temperatures above 630 °C indicate strong acid sites (Figure S3(a)). The presence of weak, medium, and strong acid sites on the catalyst surface could promote deoxygenation. In addition, the CO_2-TPD profiles indicated that the addition of K_2O promotes the formation of basic sites of several strengths, including weak, medium, and strong, which significantly contribute to the overall catalytic performance of the catalyst (Figure S3(b)).

Figure 7 shows that the incorporation of K_2O into the Cu-MOF catalyst facilitated the conversion of LFAs into shorter-chain hydrocarbon products. The unmodified Cu-MOF catalyst, lacking K_2O impregnation, exhibited lower basicity and demonstrated higher selectivity toward green diesel than Cu-MOF catalysts impregnated with 3, 5, and 10 wt% K_2O. Notably, the Cu-MOF/3-K_2O catalyst exhibited significant selectivity toward biogasoline (29%) and biokerosene (57%), while suppressing the formation of green diesel (14%). However, increasing the K_2O concentration did not significantly improve the composition ratio of biogasoline, biokerosene, and green diesel. Accordingly, the increase in K_2O concentration was not significant in increasing the composition ratio of biogasoline, biokerosene, and green diesel. For Cu-MOF/5-K_2O, the selectivity toward biogasoline and biokerosene was 36% and 47%, respectively, while Cu-MOF/10-K_2O exhibited biogasoline and biokerosene selectivity of 29% and 53%, respectively.

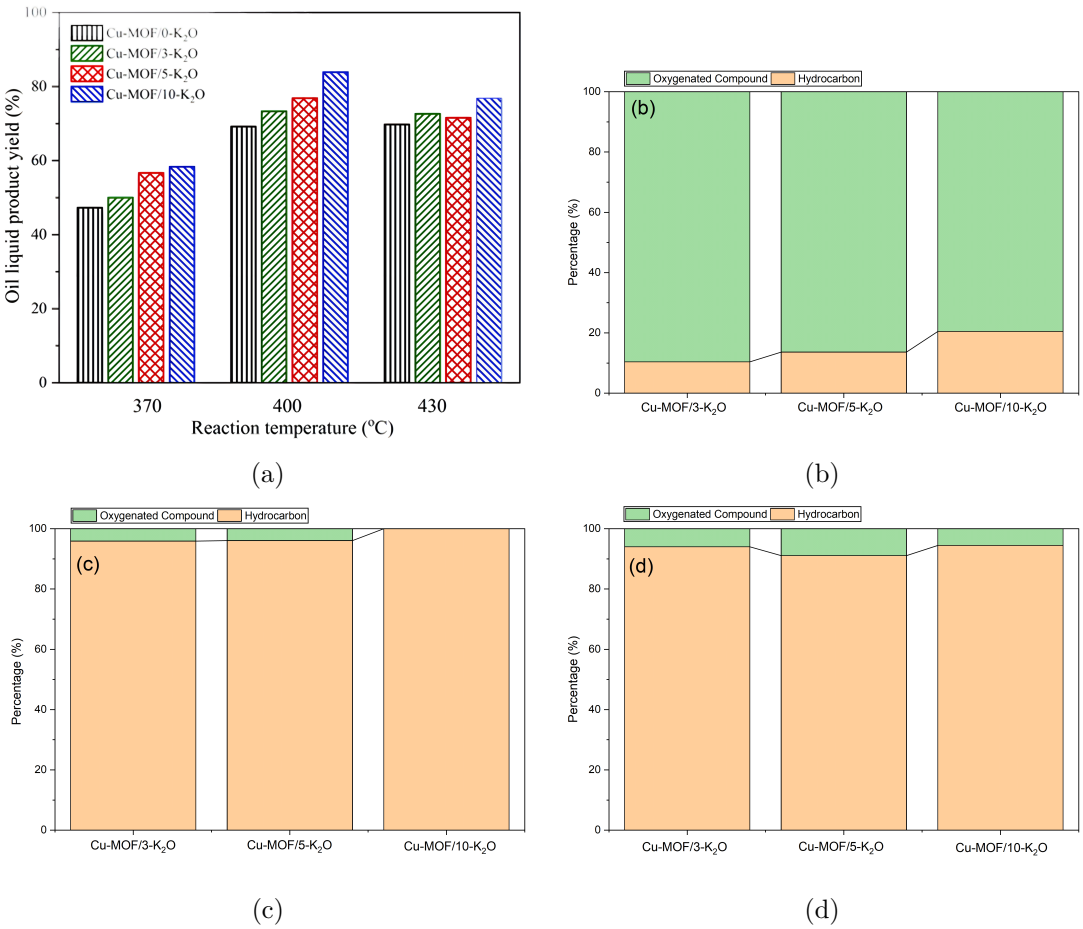

Figure 6 (a) Yield of OLP at different reaction temperatures and distribution of OLP components with the synthesized catalyst at (b) 370 °C, (c) 400 °C, and (d) 430 °C. Reaction Cond.: 272 g WCO, 15 g catalyst, 1 h, 8 °C/min

Nevertheless, the impregnation of K_2O in Cu-MOF led to the production of shorter-chain hydrocarbons. These findings support the previous report that catalysts with higher basicity tend to favor the production of lighter biofuels such as biogasoline and biokerosene (Hafriz et al., 2022; Asikin-Mijan et al., 2016). Additionally, base catalysts such as like Na_2CO_2 have been reported to convert WCO into aviation fuel fractions (Li et al., 2018).

WCO undergoes thermal decomposition of triglycerides and fatty acid molecules to produce oxygenated products. In the second stage, these oxygenated products react over a catalyst, forming saturated or unsaturated hydrocarbon compounds. In addition, at elevated temperatures, triglycerides in WCO undergo hydrogen abstraction, synthesizing dienes. During the deoxygenation of fatty acids, decarbonylation (DCO) and decarboxylation (DCO_2) may occur, as illustrated in Figure 8. Deoxygenation cracking can occur under atmospheric pressure because the reaction does not use simultaneous addition of hydrogen. According to the results, CuO and Cu_2O derived from Cu-MOF play a significant role in the deoxygenation reaction, whereas K_2O facilitates the conversion of long-chain hydrocarbons to shorter-chain hydrocarbons. The synergistic effect of Cu-MOF and K_2O could enhance the selectivity of biofuel products.

In addition, the Diels-Alder process produces cycloolefins (C_nH_{2n-2}) from olefins (C_nH_{2n}) and dienes, which subsequently form cyclic and aromatic hydrocarbons. Hydrogen (H_2) is incorporated into the double bonds of cycloolefins to produce saturated cyclo-paraffins (C_nH_{2n}). Several alkynes (C_nH_{2n-2}) and aromatics (C_nH_n) are observed in the liquid products, which can be formed through dehydrogenation reactions (Chansiriwat et al., 2022). Specifically, it facilitates the water-gas shift reaction by acting as an active site for the conversion of the reaction:

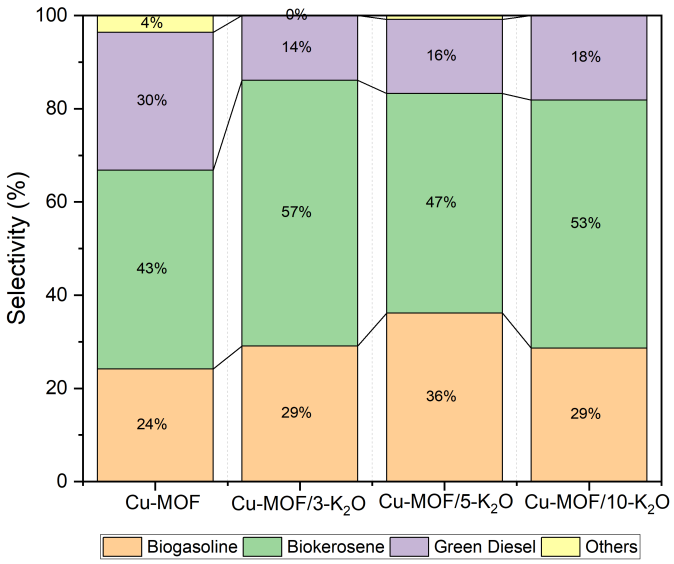

Figure 7 OLP biofuel selectivity using various synthesized catalysts Reaction conditions: 272 g WCO, 15 g catalyst, 400 °C

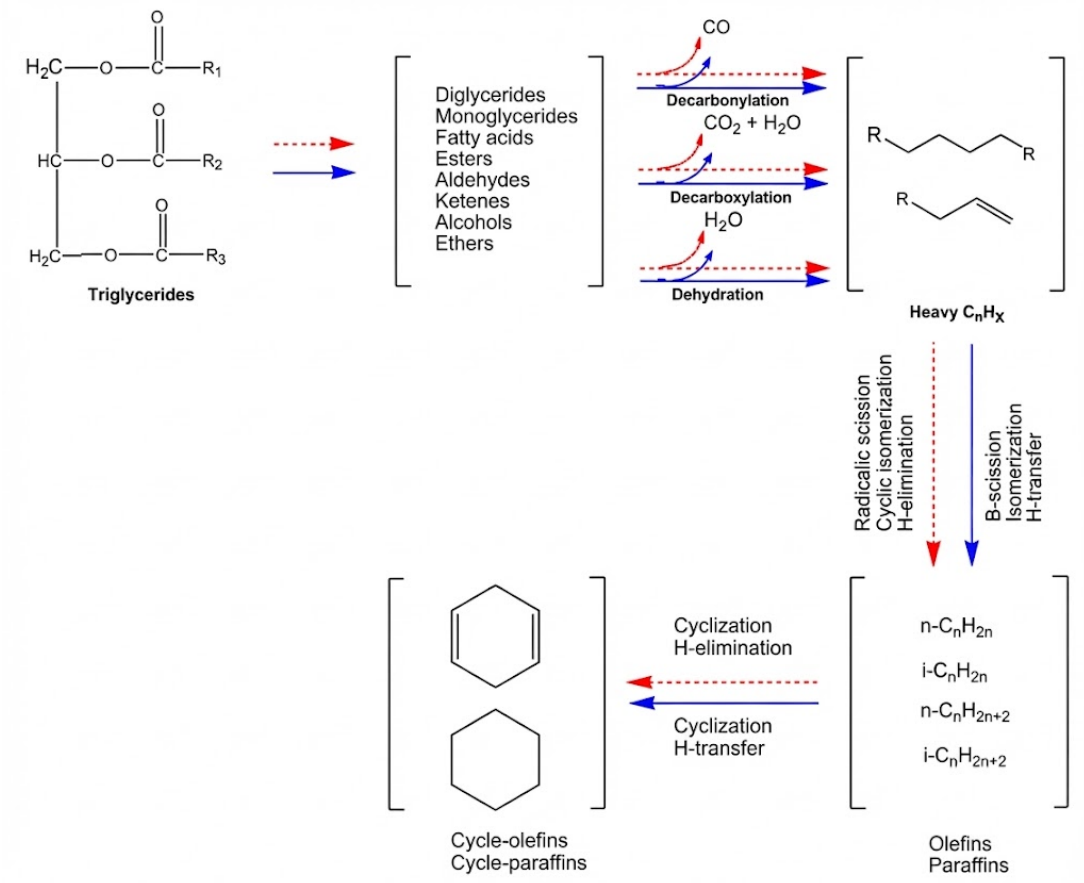

Figure 8 Reaction scheme of triglyceride conversion to hydrocarbons

$$CO + H_2O \rightarrow H_2 + CO_2 \quad (6)$$

This inherent catalytic characteristic makes the deoxygenation process more cost-effective by drastically lowering the need for outside hydrogen sources. This catalyst increases the overall

hydrocarbon formation efficiency while guaranteeing a sustainable hydrogen supply for deoxygenation reactions by encouraging in situ hydrogen production.

The Cu-MOF/K_2O catalyst developed in this study demonstrates a balanced performance compared with conventional hydrotreating and cracking catalysts. This catalyst achieved near-complete conversion into hydrocarbons (>99.9%) without an external H_2 supply. Traditional hydrodeoxygenation catalysts, such as sulfided Co-Mo or Ni-Mo, typically require high hydrogen pressures to achieve comparable deoxygenation efficiencies (Mussa et al., 2024). This indicates This indicates that oxygen removal over Cu–MOF/K_2O proceeds efficiently via decarboxylation, decarbonylation, and dehydration pathways under inert conditions, consistent with the presence of CuO/Cu_2O phases and synergistic acid–base functionality introduced by K_2O.

3.2.4 Physicochemical Properties of Feedstock and Product

The WCO characterization involved testing its FFA content, moisture content, density, viscosity, calorific value, and flash point. As detailed in the methodology section, the WCO used in this study underwent a pretreatment process with earth bleaching. FFA content testing is crucial because high FFA levels can increase saponification reactions, reduce biofuel yield, and raise viscosity (Alias et al., 2018). The FFA content was analyzed using the alkalimetric method, yielding a value of 0.7%. This value is considered suitable for the PCC process, preventing saponification, as supported by previous studies indicating a maximum FFA threshold of 2% for effective transesterification (Banerjee and Chakraborty, 2009).

The moisture content of the feedstock was determined to be 0.0325%. Water in the oil sample has detrimental effects as it can trigger hydrolysis reactions, reducing biodiesel yield and increasing catalyst consumption (Yaakob et al., 2013). Additionally, water contributes to soap and foam formulation, further elevating viscosity. The maximum allowable moisture content for biofuel production is 0.050% according to the ASTM D6751 standard. The WCO used in this study meets this requirement because its moisture content falls below the specified threshold.

The physicochemical characterization of the product revealed that the calorific value of OLP (43.051 MJ/kg) was higher than that of WCO (37.6 MJ/kg). The calorific value of OLP is comparable to that of fossil diesel (42-44 MJ/kg). The calorific value of biofuels is a critical parameter as it directly impacts the energy content and fuel efficiency. When assessing the performance and appropriateness of biofuels as substitutes for traditional fossil fuels, a higher calorific value indicates a higher energy yield per unit mass of the fuel. The calorific value influences the heating efficiency, combustion characteristics, and overall energy output of the fuel during use. Fuels with a higher calorific value are preferred in industries such as power generation and transportation that require high energy content for combustion. Therefore, optimizing catalytic processes to enhance the calorific value of biofuels, as demonstrated with OLP, is crucial for improving biofuel performance and competitiveness in the energy market (Demirbas, 2009). This value shows that the oxygenated hydrocarbon content in OLP contributes to its superior energy content compared to WCO. The increased calorific value of OLP can be attributed to the reduction of oxygenated compounds through the Cu-MOF-facilitated deoxygenation process, which contributes to oxygen removal and an increased carbon-to-oxygen ratio. These compounds are more favorable for fuel applications because they typically have a higher energy density due to their reduced oxygen concentration (Knothe, 2008)

Additionally, a notable rise in viscosity was noted. The reduction in kinematic viscosity, flash point, and density following the cracking process (Table 4) can be attributed to the breakdown of larger molecules into smaller, lighter fractions and the removal of oxygen, which weakens intermolecular interaction (Kasar et al., 2020). These results are consistent with earlier research on biomass-based feedstocks, which showed that the chemical makeup of OLP significantly impacts the physical and chemical characteristics of the fuels. Compounds with shorter hydrocarbon chains and less oxygen have lower density and viscosity. Additionally, this study shows that the viscosity and flash point values comply with the ASTM standards.

Furthermore, the flashpoint of OLP indicates that the biokerosene-rich fraction (39 °C) ex-

ceeds the minimum requirement specified in ASTM D1655 for A-1 jet fuel (38 °C), meeting key safety criteria for aviation applications. These comparisons demonstrate that the biogasoline, biokerosene, and green diesel fractions produced over Cu–MOF/K_2O not only fall within standard carbon number ranges but also comply with ASTM fuel standards' critical physicochemical requirements.

Table 4 Physicochemical properties of WCO and OLP

Physicochemical properties	WCO	OLP	ASTM limit
Density (g/cm^3) @25°C	0.908	0.811	–
Kinematic viscosity (mm^2/s) @25°C	44.053	5	1.9–6
Caloric value (MJ/kg)	37.6	43.051	–
Flashpoint (°C)	302	39	38–72 (Kerosene)

4. Conclusions

This study investigates the conversion of WCO into biofuel using a Cu-MOF/K_2O catalyst. The synthesis and characterization of these catalysts through FTIR, XRD, SEM, and other techniques confirmed the successful doping of K_2O onto Cu-MOF, which enhanced the thermal stability and deoxygenation properties of the catalyst. The Cu-MOF/10- K_2O variant, which achieved the highest hydrocarbon yield (>99.9%) at an optimal reaction temperature of 400°C, exhibited superior catalytic performance. The catalysts facilitated the PCC of WCO, leading to a reduction in oxygenated compounds and the formation of high-quality biofuels, including biokerosene, biogasoline, and green diesel, with favorable physicochemical properties meeting ASTM biofuel standards. These improvements indicate the feasibility of using WCO as a feedstock for biofuel production, offering significant environmental and economic benefits. However, the prolonged catalyst synthesis and relatively low yield present challenges for industrial applications. Further research is needed to assess broader use in sustainable biofuel production.

Acknowledgements

The authors would like to thank the Ministry of Education and Culture, Research and Technology through Basis Informasi Penelitian dan Pengabdian kepada Masyarakat (BIMA) – Implementation of the State University Operational Assistance Program Regular Fundamental Research (Master Contract Number: 038/E5/PG.02.00.PL/2024, dated June 11, 2024; Researcher Contract Number: 1782/PKS/ITS/2024, dated June 12, 2024) for financial support.

Author Contributions

Tri Widjaja conceived the research framework, supervised the overall study, and provided substantial guidance in refining the manuscript. Ali Altway contributed to the methodology development, data analysis, and interpretation of the research findings. Shofia Khoirunnisa was' was responsible for conducting the literature review, compiling relevant data, and drafting the initial manuscript. Dinda Amelia Nurhanifa performed the experimental work, collected the primary data, and analyzed the results. Mahfud Mahfud assisted in data validation, provided technical expertise, and supported manuscript revision. Hendro Juwono contributed to the theoretical background, critical discussion, and academic writing improvement. Joni Prasetyo performed the statistical analysis, supported the interpretation of the findings, and contributed to the revision of the manuscript. Deliana Dahnum critically reviewed the research framework, contributed intellectual input, and substantially revised the manuscript. Aisyah Alifatul Zahidah Rohmah assisted in preparing figures and tables, organizing references, and editing the manuscript. All authors have read and approved the final version of the manuscript.

Conflict of Interest

The authors have no conflicts of interest to declare.

References

Alias, N. I., Kumar, J. K., & Zain, S. M. (2018). Characterization of waste cooking oil for biodiesel production. *Jurnal Kejuruteraan*, *1*(2), 79–83. https://doi.org/10.17576/jkukm-2018-si1(2)-10

Asikin-Mijan, N., Lee, H., Juan, J., Noorsaadah, A., Abdulkareem-Asultan, G., Arumugam, M., & Taufiq-Yap, Y. (2016). Waste clamshell-derived cao supported co and w catalysts for renewable fuels production via cracking-deoxygenation of triolein. *Journal of Analytical and Applied Pyrolysis*, *120*, 110–120. https://doi.org/10.1016/j.jaap.2016.04.015

Associates, L. W. (2020). Statistical review of world energy [Retrieved from https://www.bp.com/en/global/corporate/energy-economics/statistical-review-of-world-energy.html].

Baharudin, K. B., Abdullah, N., Taufiq-Yap, Y. H., & Derawi, D. (2020). Renewable diesel via solventless and hydrogen-free catalytic deoxygenation of palm fatty acid distillate. *Journal of Cleaner Production*, *274*, 122850. https://doi.org/10.1016/j.jclepro.2020.122850

Banchapattanasakda, W., Asavatesanupap, C., & Santikunaporn, M. (2023). Conversion of waste cooking oil into bio-fuel via pyrolysis using activated carbon as a catalyst. *Molecules*, *28*, 3590.

Banerjee, A., & Chakraborty, R. (2009). Parametric sensitivity in transesterification of waste cooking oil for biodiesel production—a review. *Resources, Conservation and Recycling*, *53*(9), 490–497. https://doi.org/10.1016/j.resconrec.2009.04.003

Battauz, F. D., Zoppas, F. M., Sacco, N. A., & Marchesini, F. A. (2025). Resins-supported cu catalysts for the fenton-like oxidation of phenol from water. *Desalination and Water Treatment*, *321*, 101009.

Binaeian, E., Maleki, S., Motaghedi, N., & Arjmandi, M. (2019). Study on the performance of cd2+ sorption using dimethylethylenediamine-modified zinc-based mof (zif-8-mmen): Optimization of the process by rsm technique. *Separation Science and Technology*. https://doi.org/10.1080/01496395.2019.1655056

Cárdenas, J., Orjuela, A., Sánchez, D. L., Narváez, P. C., Katryniok, B., & Clark, J. (2021). Pretreatment of used cooking oils for the production of green chemicals: A review. *Journal of Cleaner Production*, *289*, 125129. https://doi.org/10.1016/j.jclepro.2020.125129

Chansiriwat, W., Wantala, K., Khunphonoi, R., Khemthong, P., Suwannaruang, T., & Rood, S. C. (2022). Enhancing the catalytic performance of calcium-based catalyst derived from gypsum waste for renewable light fuel production through a pyrolysis process: A study on the effect of magnesium content. *Chemosphere*, *292*, 133516. https://doi.org/10.1016/j.chemosphere.2022.133516

Chueaphetr, R., Suwannaruang, T., Khunphonoi, R., Khemthong, P., & Wantala, K. (2023). Enhancing deoxygenation of waste cooking palm oil over cao-mgo catalyst modified by k2o for green bio-fuel. *Fuel*, *354*. https://doi.org/10.1016/j.fuel.2023.129350

Demirbas, A. (2009). *Biofuels: Securing the planet's future energy needs*. Springer-Verlag.

Dewi, R., & Agarta, V. (2023). 11 negara penghasil sawit terbesar di dunia 2023, indonesia nomor 1 [Retrieved May 20, 2023 from https://koran.tempo.co/read/ekonomi-dan-bisnis/482145/11-negara-penghasil-sawit-terbesar-di-dunia-2023-indonesia-nomor-1].

Edeh, I., Overton, T., & Bowra, S. (2021). Renewable diesel production by hydrothermal decarboxylation of fatty acids over platinum on carbon catalyst. *Biofuels*, *12*(8), 945–952. https://doi.org/10.1080/17597269.2018.1560554

French, M. (2024). Today in energy [Retrieved December 23, 2025 from https://www.eia.gov/todayinenergy/].

Garside, M. (2019). Primary energy demand worldwide from 2015 to 2040, by fuel type in million barrels of oil equivalent per day [Retrieved from https://www.statista.com/statistics/265598/consumption-of-primary-energy-worldwide/].

Hafriz, R., Shafizah, I. N., Arifin, N., Maisarah, A., Salmiaton, A., & Shamsuddin, A. (2022). Comparative, reusability and regeneration study of potassium oxide-based catalyst in deoxygenation reaction of wco. *Energy Conversion and Management: X*, *13*, 100173. https://doi.org/10.1016/j.ecmx.2021.100173

Hoque, M. A., Guzman, M. I., Selegue, J. P., & Gnanamani, M. K. (2022). Chemical state of potassium on the surface of iron oxides: Effect of potassium precursor concentration and calcination temperature. *Materials*, *15*, 7278. https://doi.org/10.3390/ma15207378

Jamil, U., Khoja, A. H., Liaquat, R., Naqvi, S. R., Omar, W. N., & Amin, N. A. (2020). Copper and calcium-based metal organic framework (mof) catalyst for biodiesel production from waste cooking oil: A process optimization study. *Energy Conversion and Management*, *215*. https://doi.org/10.1016/j.enconman.2020.112934

Jawad, K. A., Saed, U. A., & Alwan, H. H. (2020). Synthesis of nano platinum-tungsten supported on gamma-alumina catalyst. *IOP Conference Series: Materials Science and Engineering*, *928*, 022103. https://doi.org/10.1088/1757-899X/928/2/022103

Jeon, K.-W., Cho, J.-W., Park, H.-R., Na, H.-S., Shim, J.-O., Jang, W.-J., & Roh, H.-S. (2020). One-pot sol–gel synthesis of a como catalyst for sustainable biofuel production by solvent- and hydrogen-free deoxygenation: Effect of the citric acid ratio. *Sustainable Energy & Fuels*, *4*(6), 2841–2849. https://doi.org/10.1039/D0SE00159G

Jiang, H., Wang, Q., Wang, H., Chen, Y., & Zhang, M. (2016). Temperature effect on the morphology and catalytic performance of co-mof-74 in low-temperature nh3-scr process. *Catalysis Communications*, *80*, 24–27. https://doi.org/10.1016/j.catcom.2016.03.013

Kasar, P., Sharma, D., & Ahmaruzzaman, M. (2020). Thermal and catalytic decomposition of waste plastics and its co-processing with petroleum residue through pyrolysis process. *Journal of Cleaner Production*, *265*. https://doi.org/10.1016/j.jclepro.2020.121639

Knothe, G. (2008). Designer biodiesel: Optimizing fatty ester composition to improve fuel properties. *Energy & Fuels*, *22*, 1358–1364. https://doi.org/10.1021/ef700639e

Laksmono, N., Paraschiv, M., Loubar, K., & Tazerout, M. (2013). Biodiesel production from biomass gasification tar via thermal/catalytic cracking. *Fuel Processing Technology*, *106*, 776–783. https://doi.org/10.1016/j.fuproc.2012.10.016

Li, F., Jiang, J., Liu, P., Zhai, Q., Wang, F., Hse, C.-Y., & Xu, J. (2018). Catalytic cracking of triglycerides with a base catalyst and modification of pyrolytic oils for production of aviation fuels. *Sustainable Energy & Fuels*, *2*, 1206–1215. https://doi.org/10.1039/C7SE00505A

Long, F., Zhai, Q., Liu, P., Cao, X., Jiang, X., Wang, F., & Xu, J. (2020). Catalytic conversion of triglycerides by metal-based catalysts and subsequent modification of molecular structure by zsm-5 and raney ni for the production of high-value biofuel. *Renewable Energy*, *157*, 1072–1080. https://doi.org/10.1016/j.renene.2020.05.117

Mohammed, S. T., Hamad, K. I., Gheni, S. A., Aqar, D. Y., Ahmed, S. M., Mahmood, M. A., & Abdullah, G. H. (2022). Enhancement of stability of pd/ac deoxygenation catalyst for hydrothermal production of green diesel fuel from waste cooking oil. *Chemical Engineering Science*, *251*, 117489. https://doi.org/10.1016/j.ces.2022.117489

Murthy, H. A., Zeleke, T. D., Tan, K., Ghotekar, S., Alam, M. W., Balachandran, R., & Ravikumar, C. (2021). Enhanced multifunctionality of cuo nanoparticles synthesized using aqueous leaf extract of vernonia amygdalina plant. *Results in Chemistry*, *3*, 100141. https://doi.org/10.1016/j.rechem.2021.100141

Mussa, N.-S., Toshtay, K., & Capron, M. (2024). Catalytic applications in the production of hydrotreated vegetable oil (hvo) as a renewable fuel: A review. *Catalysts*, *14*(7), 452. https://doi.org/10.3390/catal14070452

Ooi, X. Y., Gao, W., Ong, H. C., Lee, H. V., Juan, J. C., Chen, W. H., & Lee, K. T. (2019). Overview on catalytic deoxygenation for biofuel synthesis using metal oxide supported catalysts. *Renewable and Sustainable Energy Reviews*, *112*, 834–852. https://doi.org/10.1016/j.rser.2019.06.031

Pikoli, S., Kunene, A., & Makhubela, B. C. (2025). Enhanced ketonic decarboxylation of fatty acids using vanadia-modified nickel on zirconia catalyst. *Sustainable Energy & Fuels*, *9*, 2738–2752. https://doi.org/10.1039/d4se01836b

Prasetyo, J., Dahnum, D., Wihadi, M. N. K., Dwiatmoko, A. A., Widjaya, R. R., Ajie, F. T., Supriadi, E., Yuwono, H., Altway, A., & Widjaja, T. (2026). Study on profiling selectivity of co-catalyst, layer double hydroxide (ldh) and metal catalyst for deoxygenation of used cooking oil (uco) to produce green fuel. *AIP Conference Proceedings*, *3380*(1), 110001. https://doi.org/10.1063/5.0313750

Putri, R. A., Aulia, A. R., Cahyani, L. R., Widharyanti, I. D., Aziz, I., Aulia, F., & Sudiyarmanto. (2025). Tuning the catalytic activity of zif-8 by ni doping for the conversion of fatty acid to diesel range hydrocarbons in solventless condition. *Journal of Industrial and Engineering Chemistry*, *147*, 318–328. https://doi.org/10.1016/j.jiec.2024.12.022

Rodiansono, Trisunaryanti, W., & Triyono. (2007). Pembuatan, karakterisasi dan uji aktivitas katalis nimo/z dan nimo/z-nb2o5 pada reaksi hidrorengkah fraksi sampah plastik menjadi fraksi bensin. *Berkala Ilmiah MIPA*, *17*(2), 43–53.

Scaldaferri, C. A., & Pasa, V. M. (2019). Production of jet fuel and green diesel range biohydrocarbons by hydroprocessing of soybean oil over niobium phosphate catalyst. *Fuel*, *245*, 458–466. https://doi.org/10.1016/j.fuel.2019.01.179

Shen, K., Chen, X., Chen, J., & Li, Y. (2016). Development of mof-derived carbon-based nanomaterials for efficient catalysis. *ACS Catalysis*, *6*(9), 5587–5903. https://doi.org/10.1021/acscatal.6b01222

Snare, M., Kubickova, I., Maki-Arvela, P., Eranen, K., & Murzin, D. Y. (2006). Heterogeneous catalytic deoxygenation of stearic acid for production of biodiesel. *Industrial & Engineering Chemistry Research*, *45*(16), 5708–5715. https://doi.org/10.1021/ie060334i

Srifa, A., Faungnawakij, K., Itthibenchapong, V., & Assabumrungrat, S. (2015). Roles of monometallic catalysts in hydrodeoxygenation of palm oil to green diesel. *Chemical Engineering Journal*, *278*, 249–258. https://doi.org/10.1016/j.cej.2014.09.106

Sun, J. K., & Xu, Q. (2014). Functional materials derived from open framework templates/precursors: Synthesis and applications. *Energy & Environmental Science*, *7*, 2071–2100. https://doi.org/10.1039/C4EE00517A

Ulfa, A. M. (2022). Indonesia surga jelantah untuk biodiesel [Retrieved May 27, 2022 from https://katadata.co.id/infografik/6290bcb52b269/indonesia-surga-jelantah-untuk-biodiesel].

Veisi, H., Karmakar, B., Tamoradi, T., Hemmati, S., Hekmati, M., & Hamelian, M. (2021). Biosynthesis of cuo nanoparticles using aqueous extract of herbal tea (stachys lavandulifolia) flowers and evaluation of its catalytic activity. *Scientific Reports*, *11*, 1983. https://doi.org/10.1038/s41598-021-81320-6

Wakoc, F. M., Reshadb, A. S., Bhaleraoa, M. S., & Gouda, V. V. (2018). Catalytic cracking of waste cooking oil for biofuel production using zirconium oxide catalyst. *IOP Conference Series: Materials Science and Engineering*, *118*.

Yaakob, Z., Mohammad, M., Alherbawi, M., Alam, Z., & Sopian, K. (2013). Overview of the production of biodiesel from waste cooking oil. *Renewable and Sustainable Energy Reviews*, *18*, 184–193. https://doi.org/10.1016/j.rser.2012.10.016

Yang, Y., Xu, D., Wu, Q., & Diao, P. (2016). Cu2o/cuo bilayered composite as a high-efficiency photocathode for photoelectrochemical hydrogen evolution reaction. *Scientific Reports*, *6*, 35158. https://doi.org/10.1038/srep35158

Yıldız, A., Goldfarb, J. L., & Ceylan, S. (2020). Sustainable hydrocarbon fuels via one-pot catalytic deoxygenation of waste cooking oil using inexpensive unsupported metal oxide catalysts. *Fuel*, *263*, 116750. https://doi.org/10.1016/j.fuel.2019.116750

Zhang, Y., Jia, Y., Li, M., & Hou, L. (2018). Influence of the 2-methylimidazole/zinc nitrate hexahydrate molar ratio on the synthesis of zeolitic imidazolate framework-8 crystals at room temperature. *Scientific Reports*, *8*, 9597. https://doi.org/10.1038/s41598-018-28015-7